THE MAS CODE: MODELING THE CORONA AND SOLAR WIND

ZORAN MIKIĆ
JON A. LINKER
PETE RILEY
ROBERTO LIONELLO
VIACHESLAV TITOV

SCIENCE APPLICATIONS INTL. CORP.
SAN DIEGO

SUPPORTED BY NSF AND NASA

Presented at the HMI/AIA Science Teams Meeting
Monterey, CA, February 13–17, 2006

MAS Model Highlights

- MAS has been around for ~ 15 years
- It is built on a rich base of experience in computational physics and the modeling of solar coronal and fusion plasmas
- Features:
  - Time-dependent resistive MHD
  - Incorporation of observed photospheric magnetic field data
  - Evolution of boundary data
  - Coronal and heliospheric components
  - Non-uniform meshes (structured)
  - 3D finite differences in spherical (r,θ,ϕ) coordinates
  - Implicit and semi-implicit time differencing
  - Comprehensive physics model including the solar wind and energy transport (radiation, parallel thermal conduction, heating, and Alfvén waves)
  - Has been used to model CMEs

MAS Code Mesh

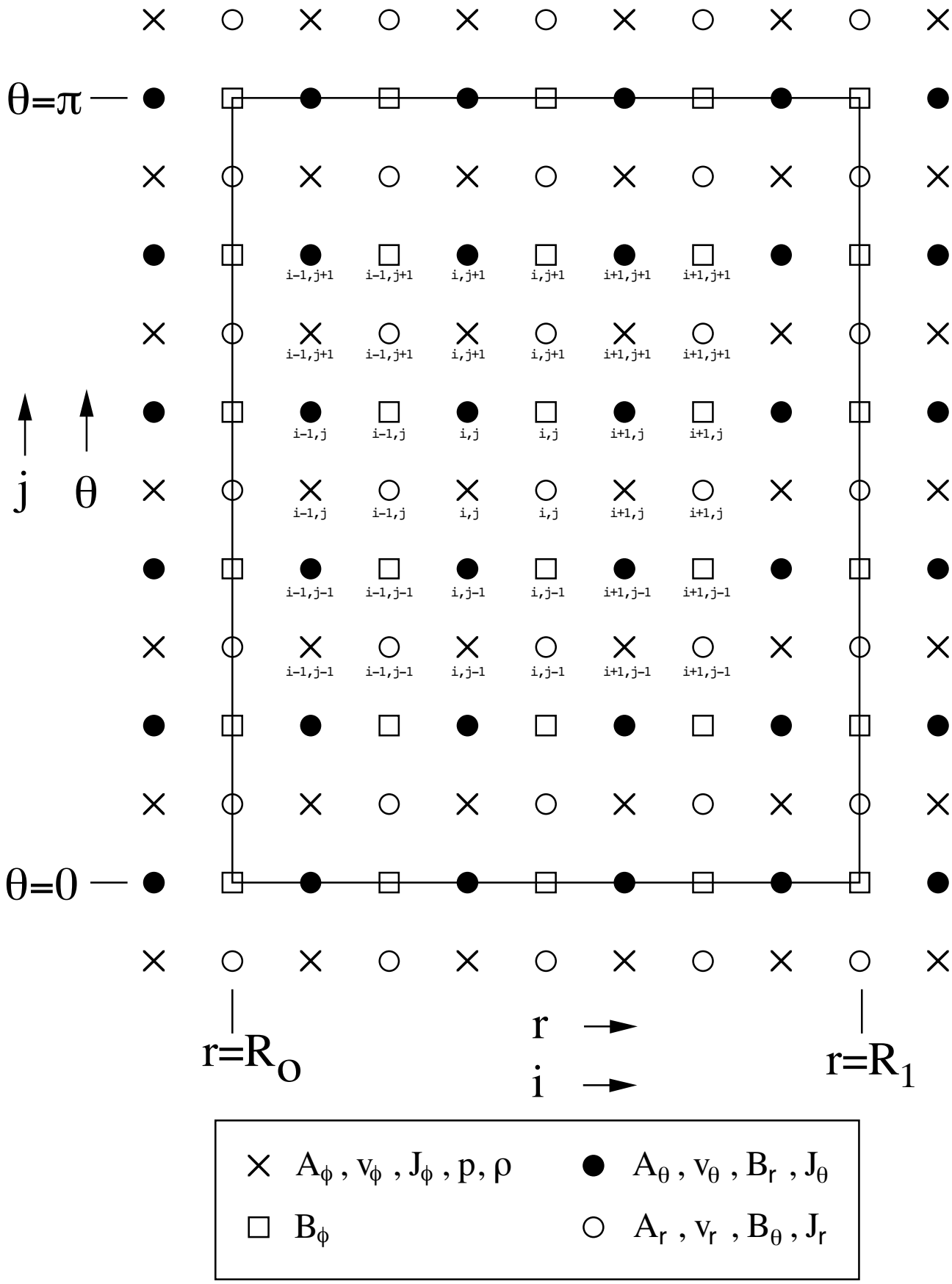

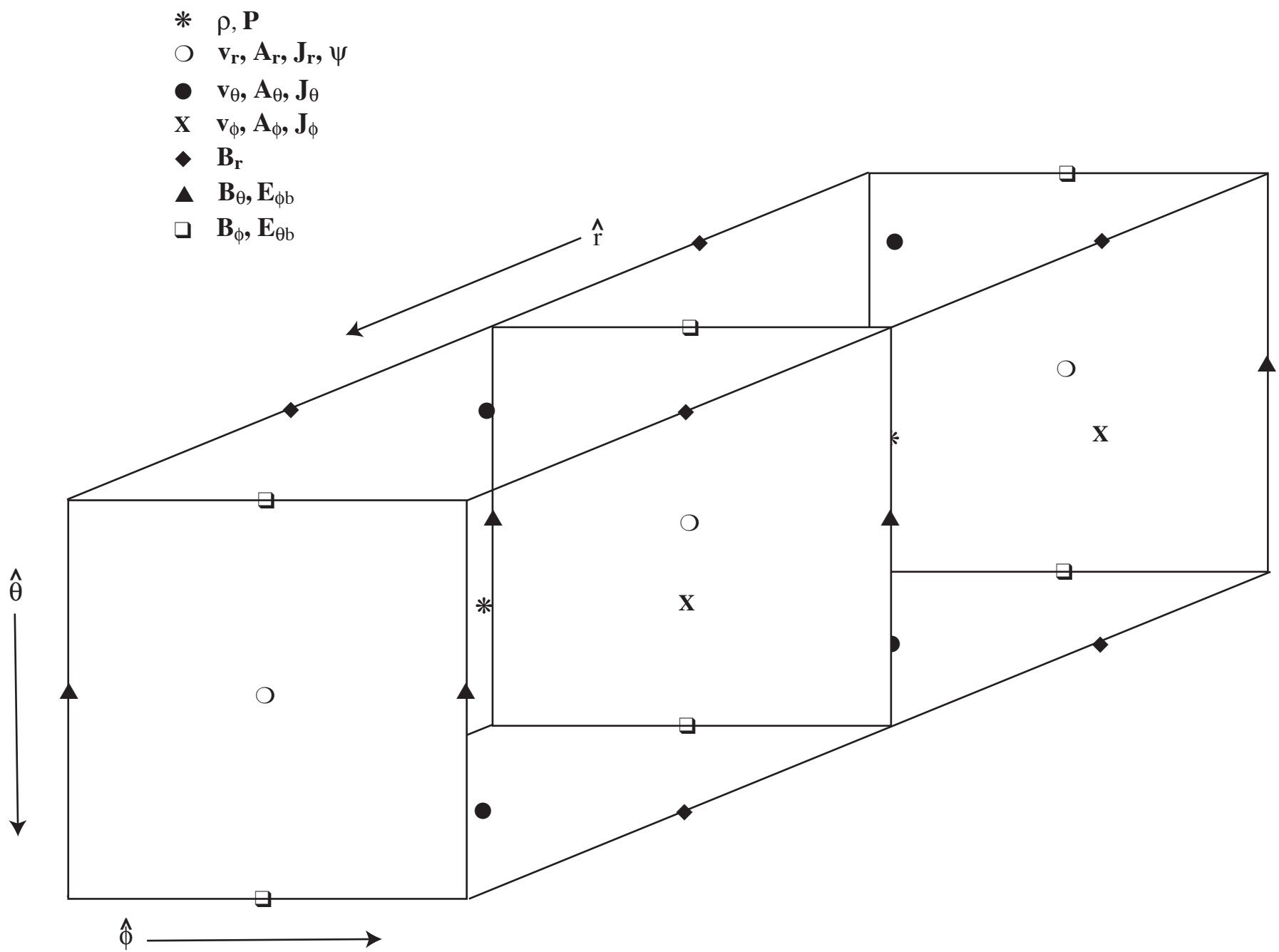
ρ, P
v_r, A_r, J_r, ψ
v_θ, A_θ, J_θ
v_φ, A_φ, J_φ
B_r
B_θ, E_φb
B_φ, E_θb
r̂
θ̂
φ̂

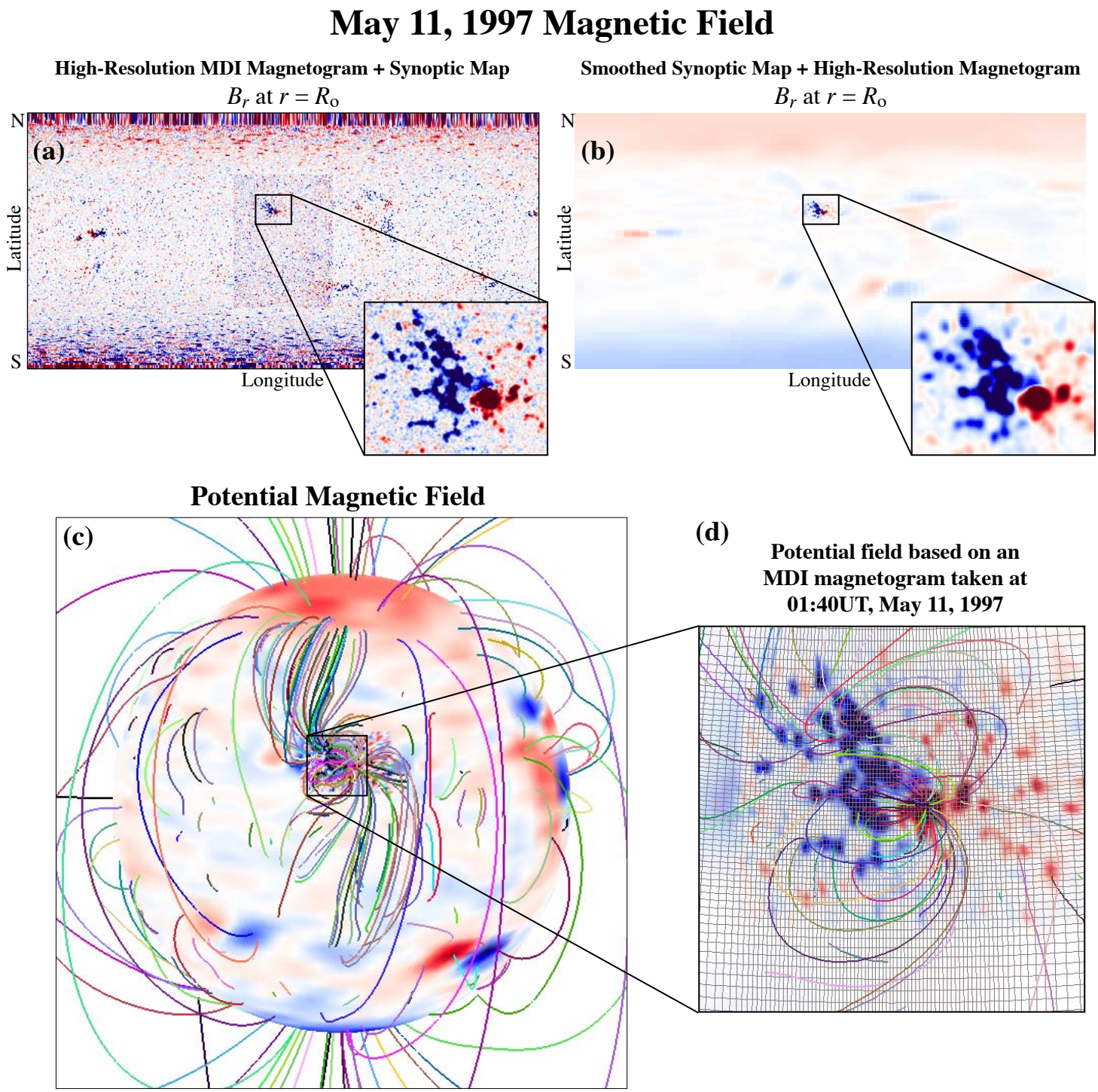

Fig. 3. The potential magnetic field on May 11, 1997 determined from MDI magnetograms and synoptic maps. (a) A high-resolution MDI magnetogram taken at 01:40UT on May 11 embedded into a high-resolution MDI synoptic map. (b) A smoothed version of the magnetic field with high resolution in the active region and smoothed fields outside the active region that is approprate for driving MHD simulations. (c) Magnetic field lines in the potential field that mathces the photospheric field in (b). (d) A zoom of the field ines in the active region, showing the computational mesh.

THE SEMI-IMPLICIT METHOD

- Only the momentum equation is modified by the addition of the semi-implicit term
- The semi-implicit term is *linear*, which simplifies inversion
- Symmetric matrices arise from the semi-implicit term $\Rightarrow$ invert with preconditioned conjugate gradient methods
- The wave terms become unconditionally stable
- The accuracy is comparable to a fully implicit scheme
- The steady-state solutions are not affected
- If Δt falls below the wave CFL limit, method is the same as an explicit method

MAS Model Highlights (Cont.)

- Written in FORTRAN 90
- Designed to run on massively parallel computers using MPI
  - IBM/SP3 + SP4 (xlf)
  - Linux & Beowulf (lf95, pgf90, Intel Fortran, pathscale)
  - Mac (Absoft and xlf)
  - SGI/Altix (ifort)
- Mesh decomposition among processors in 3D
- Dynamic allocation allows mesh size and number of processors to be selected at run time
- Restart capability using HDF files (for long runs)
- Many applications and comparisons with observational data (eclipses, IPS, *in situ* solar wind measurements, coronal holes, pB images, current sheet topology and spacecraft crossings, CMEs)
- A rich set of post-processing tools has been developed

MHD EQUATIONS
(POLYTROPIC MODEL)

$$\nabla \times \mathbf{B} = \frac{4\pi}{c}\mathbf{J}$$

$$\nabla \times \mathbf{E} = -\frac{1}{c}\frac{\partial \mathbf{B}}{\partial t}$$

$$\mathbf{E} + \frac{1}{c}\mathbf{v} \times \mathbf{B} = \eta \mathbf{J}$$

$$\frac{\partial \rho}{\partial t} + \nabla \cdot (\rho \mathbf{v}) = 0$$

$$\rho\left(\frac{\partial \mathbf{v}}{\partial t} + \mathbf{v} \cdot \nabla \mathbf{v}\right) = \frac{1}{c}\mathbf{J} \times \mathbf{B} - \nabla p + \rho \mathbf{g} + \nabla \cdot (\nu \rho \nabla \mathbf{v})$$

$$\frac{\partial p}{\partial t} + \nabla \cdot (p\mathbf{v}) = -(\gamma - 1)p\nabla \cdot \mathbf{v}$$

$\gamma = 1.05$ in the corona;
$\gamma \sim 1.5$ in the inner heliosphere

MHD EQUATIONS
(IMPROVED ENERGY TRANSPORT)

$$\nabla \times \mathbf{B} = \frac{4\pi}{c}\mathbf{J}$$

$$\nabla \times \mathbf{E} = -\frac{1}{c}\frac{\partial \mathbf{B}}{\partial t}$$

$$\mathbf{E} + \frac{1}{c}\mathbf{v} \times \mathbf{B} = \eta \mathbf{J}$$

$$\frac{\partial \rho}{\partial t} + \nabla \cdot (\rho \mathbf{v}) = 0$$

$$\rho\left(\frac{\partial \mathbf{v}}{\partial t} + \mathbf{v} \cdot \nabla \mathbf{v}\right) = \frac{1}{c}\,\mathbf{J} \times \mathbf{B} - \nabla p - \nabla p_w + \rho \mathbf{g} + \nabla \cdot (\nu \rho \nabla \mathbf{v})$$

$$\frac{\partial p}{\partial t} + \nabla \cdot (p\mathbf{v}) = (\gamma - 1)\left(-p\nabla \cdot \mathbf{v} - \nabla \cdot \mathbf{q} - n_e n_p Q(T) + H\right)$$

$$\gamma = 5/3$$

FINDING MHD SOLUTIONS

- Use line-of-sight magnetograms to deduce B_r from B_{los} at $r = R_{\mathrm{o}}$ (e.g., Kitt Peak Solar Observatory, Wilcox Solar Observatory, SOHO/MDI synoptic maps)
- Calculate a potential field matching B_r at $r = R_{\mathrm{o}}$
- Specify T and ρ on the solar surface $r = R_{\mathrm{o}}$ (e.g., uniform T_{o} and ρ_{o})
- Use characteristic boundary conditions (gas characterisitics along $\mathbf{B}$) to determine $\mathbf{v}$ at $r = R_{\mathrm{o}}$
- Set up p, ρ, and $\mathbf{v}$ from a spherically symmetric solar wind (1D Parker solution)
- Integrate 3D MHD equations in time until steady state is reached
- This gives the structure of the coronal magnetic field $\mathbf{B}$ (as well as p, ρ, $\mathbf{v}$, T)
- Compare with observations

MHD Model of the Corona and Inner Heliosphere: Overview

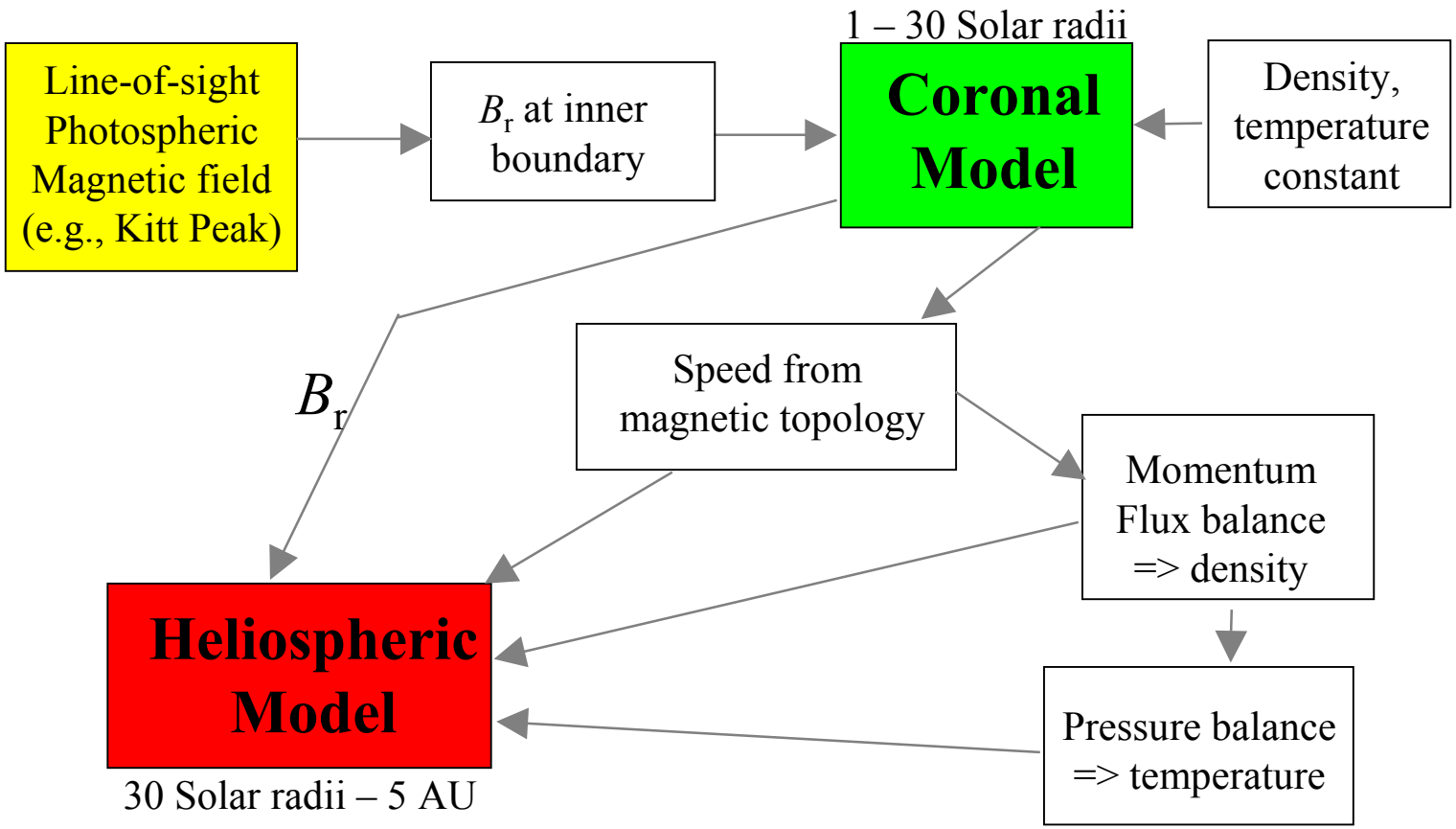

Whole Sun Month, Aug. 10 – Sep. 8, 1996

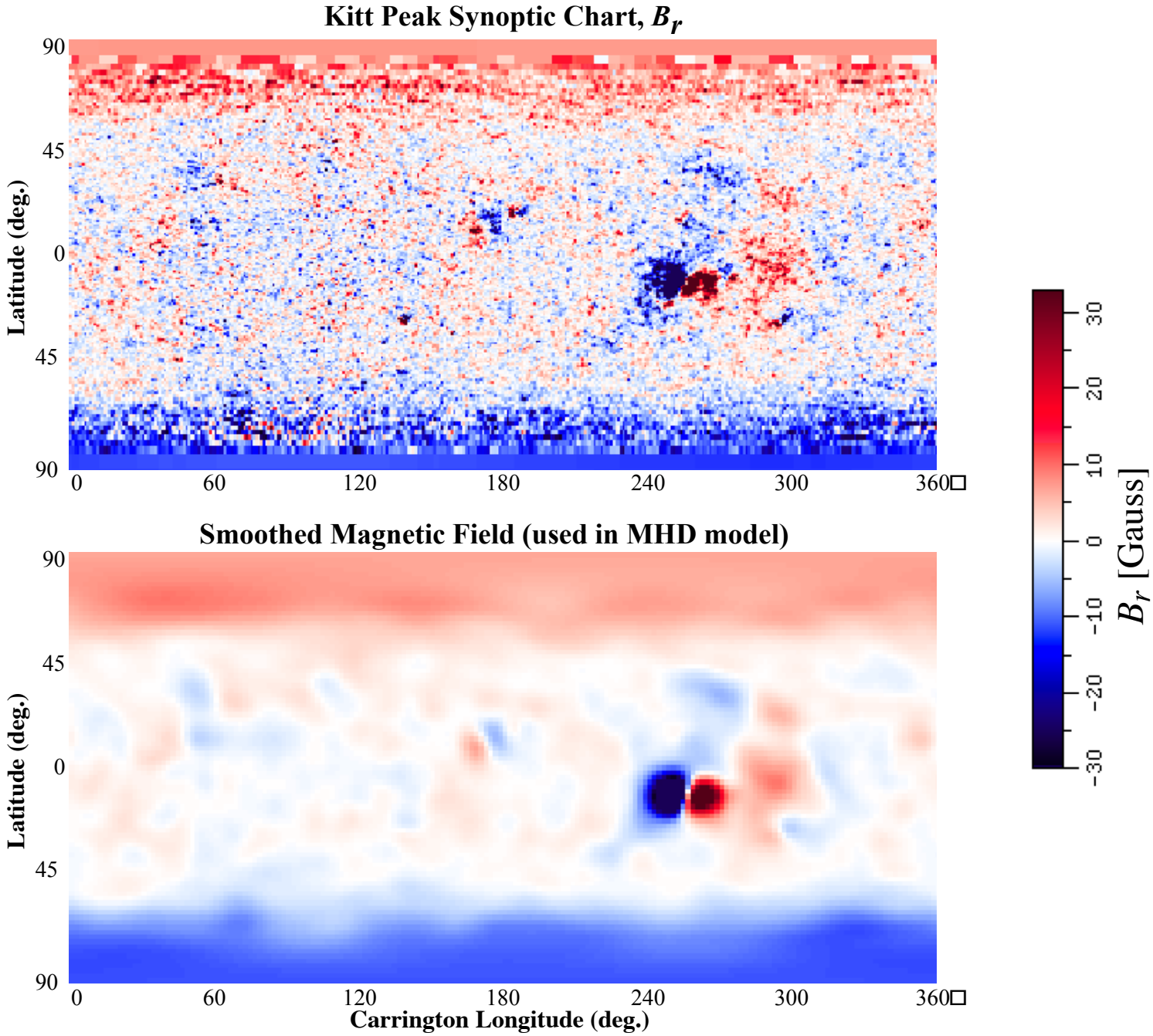

Whole Sun Month

Aug. 10 – Sep. 8, 1996

Radial Velocity
Open and Closed Field Lines

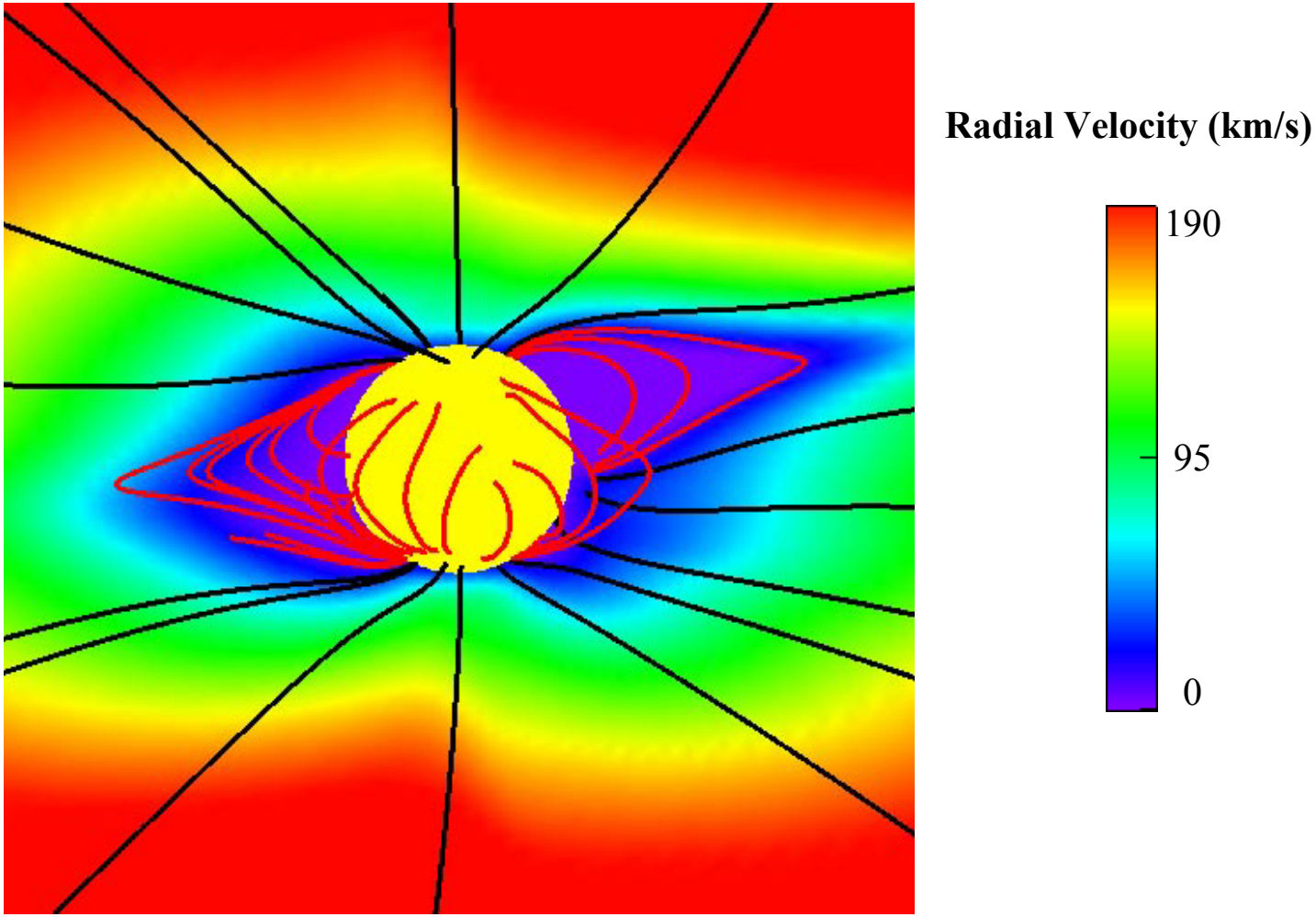

The Heliosphere During Whole Sun Month

August September 1996

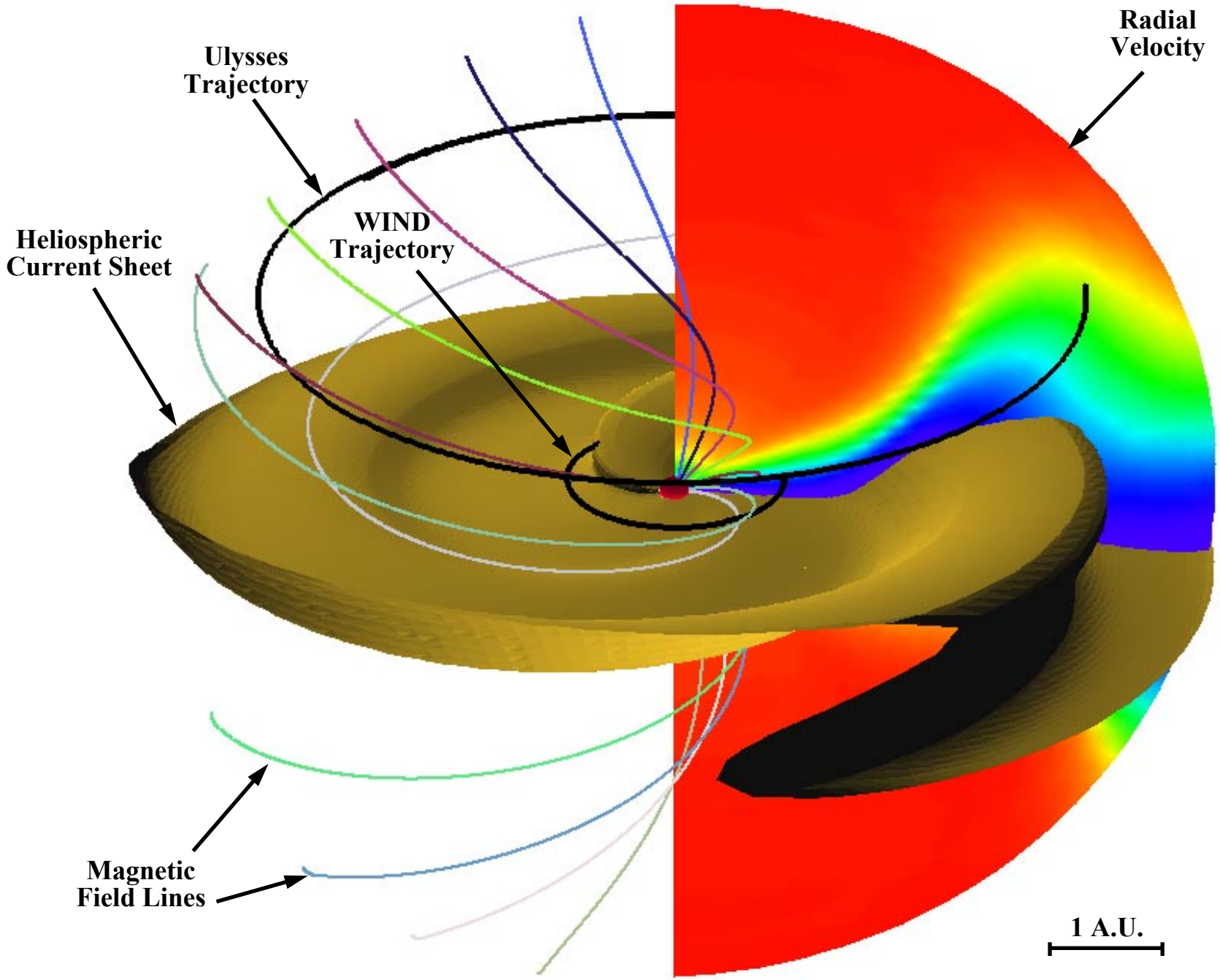

POLARIZATION BRIGHTNESS

- Light scattered off the coronal electrons is observed in coronagraphs

$$pB(\mathbf{x}) = K \int_{\text{los}} n_e(\mathbf{x} - \mathbf{x}')C(r')\, dl'$$

- $C(r)$ is a scattering function (*e.g.*, Billings 1966)
- To produce a plane-of-sky image, we apply a (radial) filter to pB ("vignetting function") and we simulate the effect of an occulting disk

MHD Modeling of the Solar Corona During Whole Sun Month

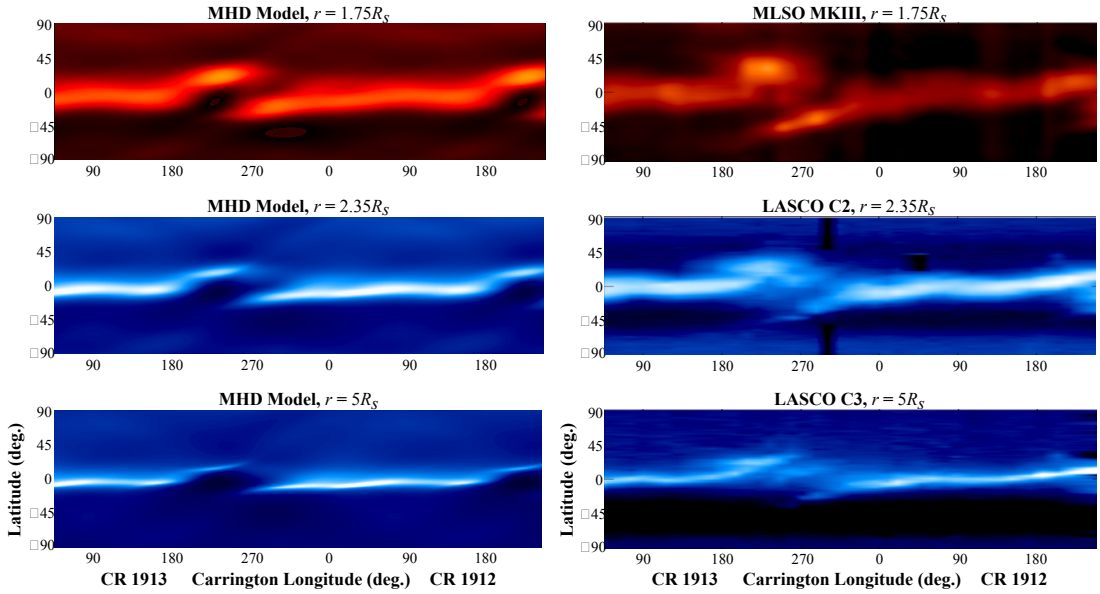

Coronal Holes

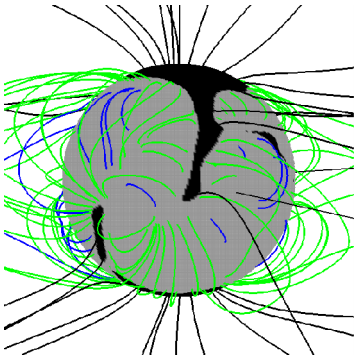

3D MHD Model (Coronal Holes)

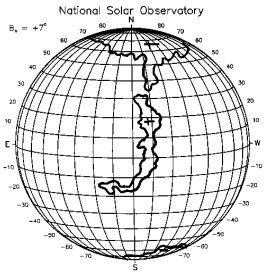

NSOKP Coronal Hole Map

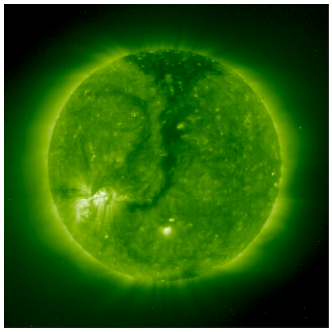

EIT Fe XII Image

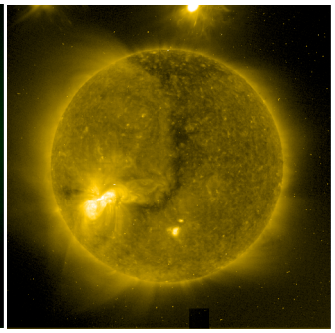

EIT Fe XV Image

Magnetic Field Lines and Heliospheric Current Sheet

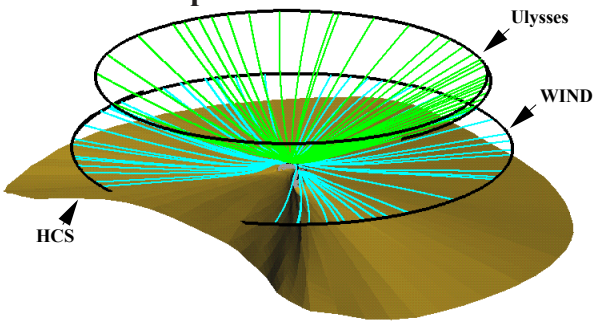

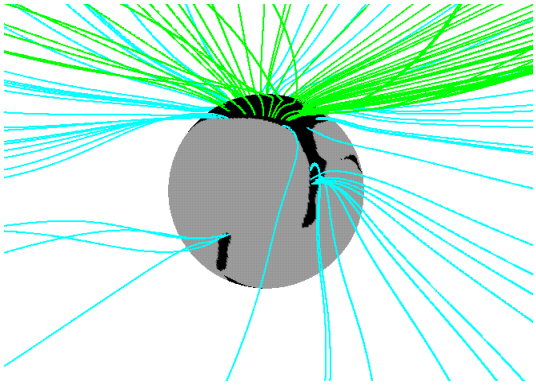

Sources of Solar Wind at the Sun Measured at Ulysses

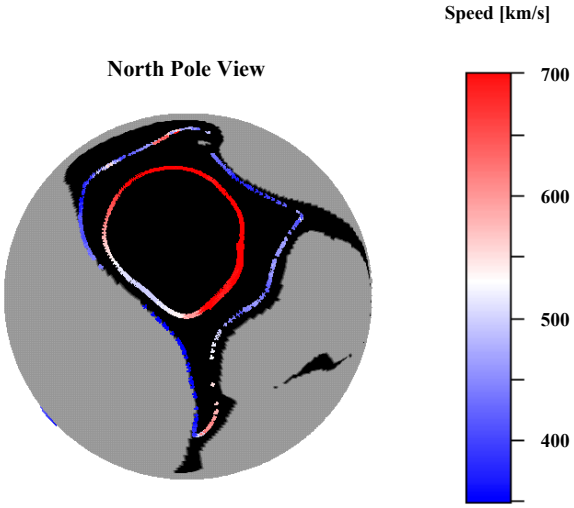

Eclipse Comparisons

Field Lines (MHD Model) | **Polarization Brightness (MHD Model)** | **Eclipse Image**

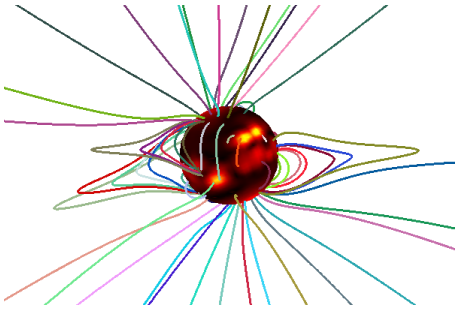
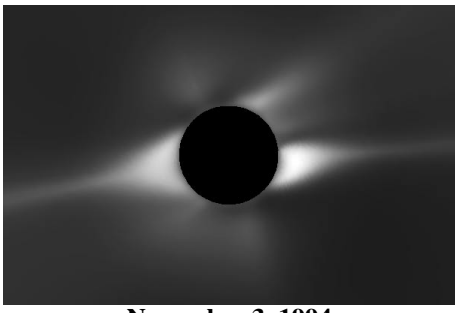
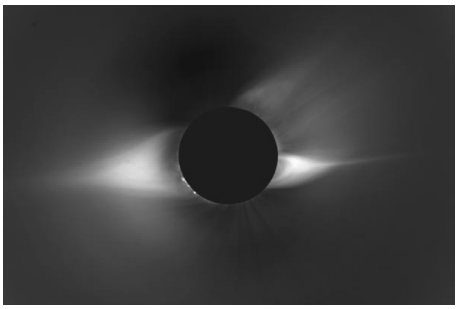

November 3, 1994

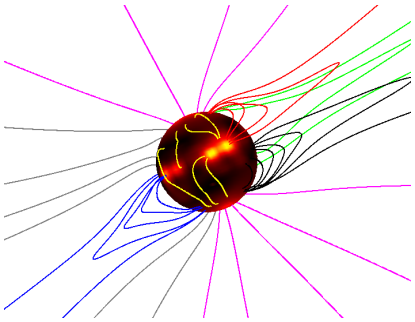
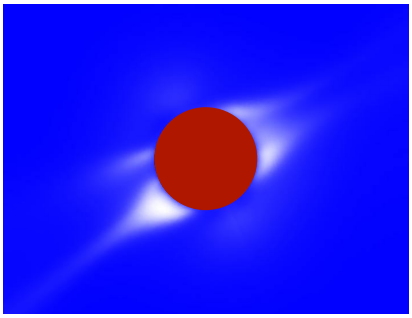
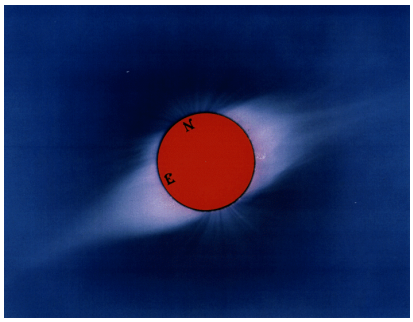

October 24, 1995

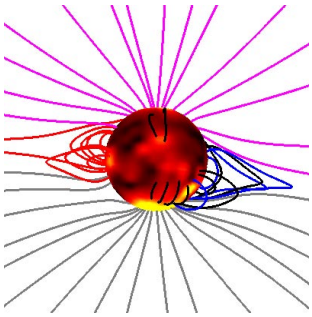
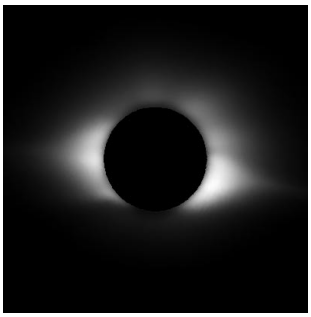


March 9, 1997

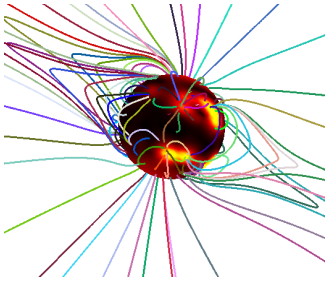
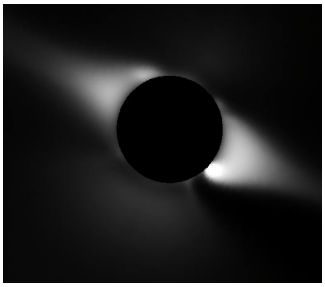
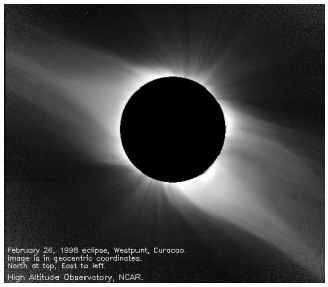

February 26, 1998

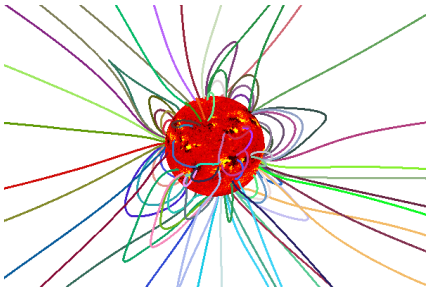
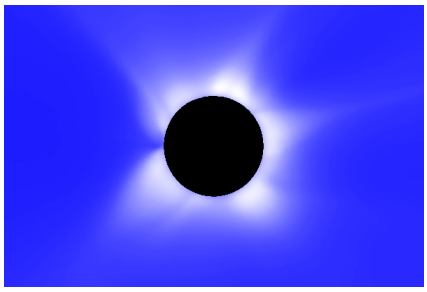


August 11, 1999

Solar Wind Velocity in the Heliosphere During Whole Sun Month (August September 1996)

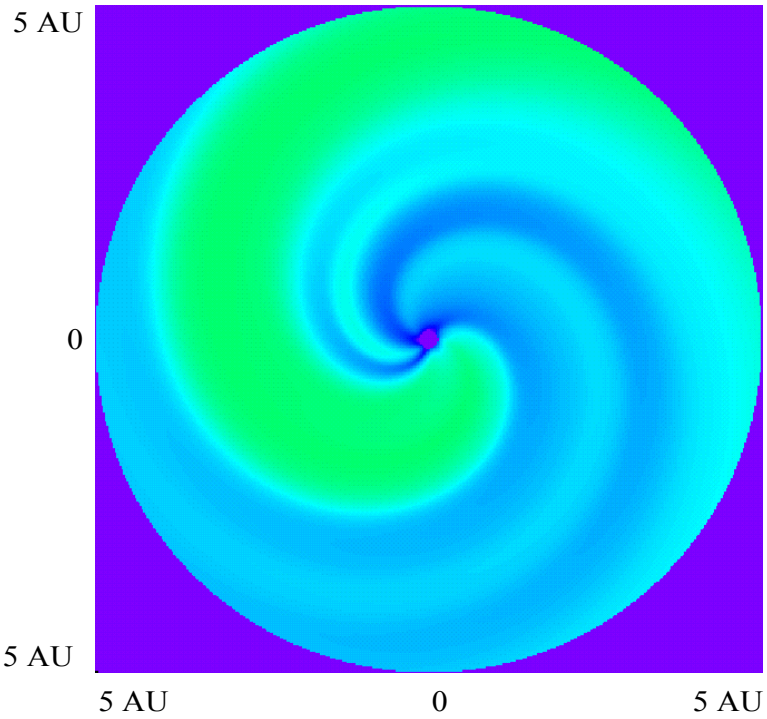

Radial Velocity in Equatorial Plane

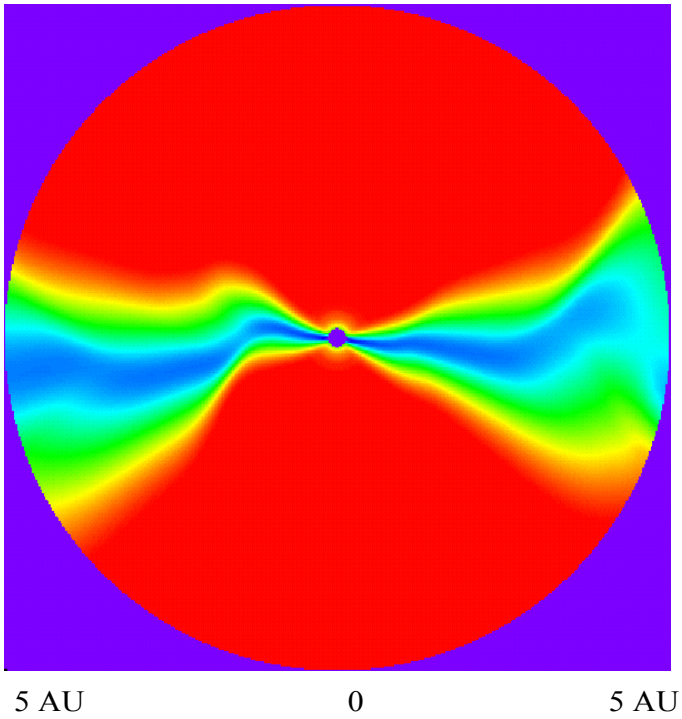

Radial Velocity in Meridional Plane

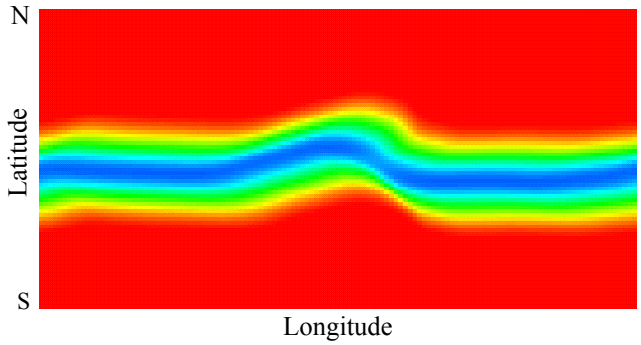

Radial Velocity at r = 1 AU

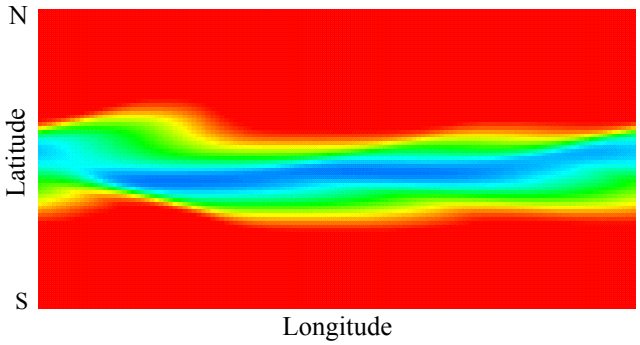

Radial Velocity at r = 4.2 AU

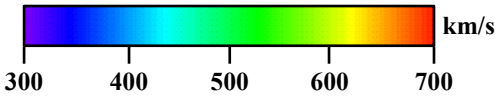

Whole Sun Month 3

Aug. 18–Sep. 14, 1999

Kitt Peak Synoptic Chart, B_r (Carrington Rotation 1953)

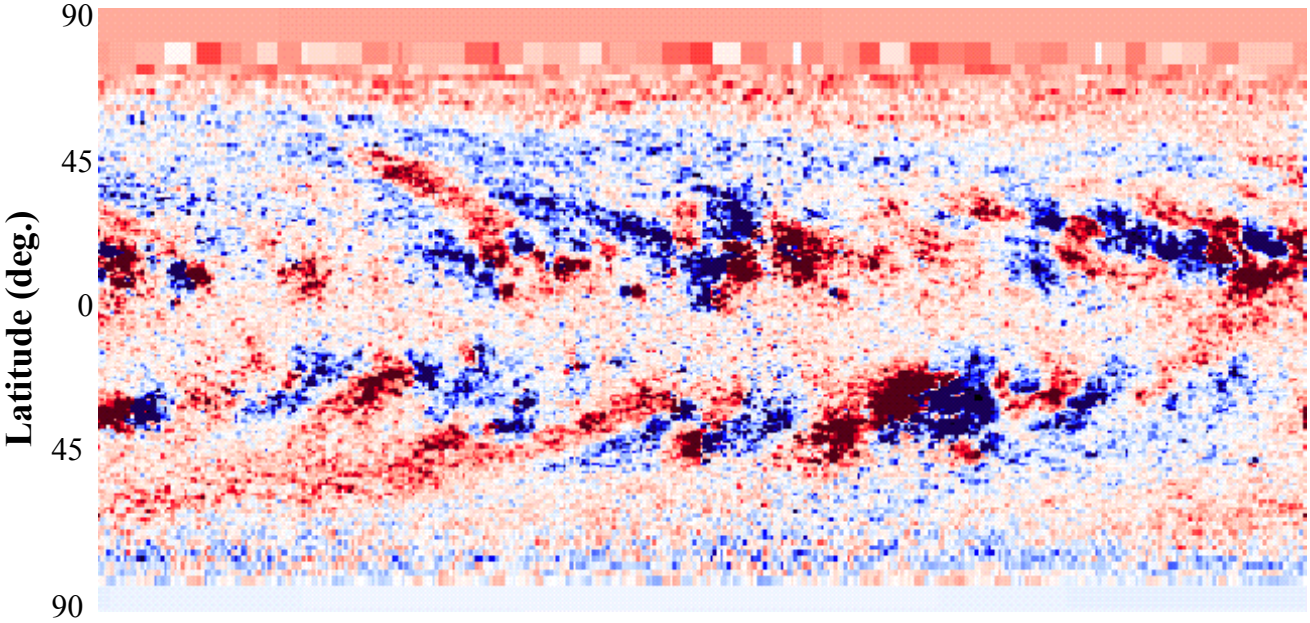

Smoothed Magnetic Field (used in MHD model)

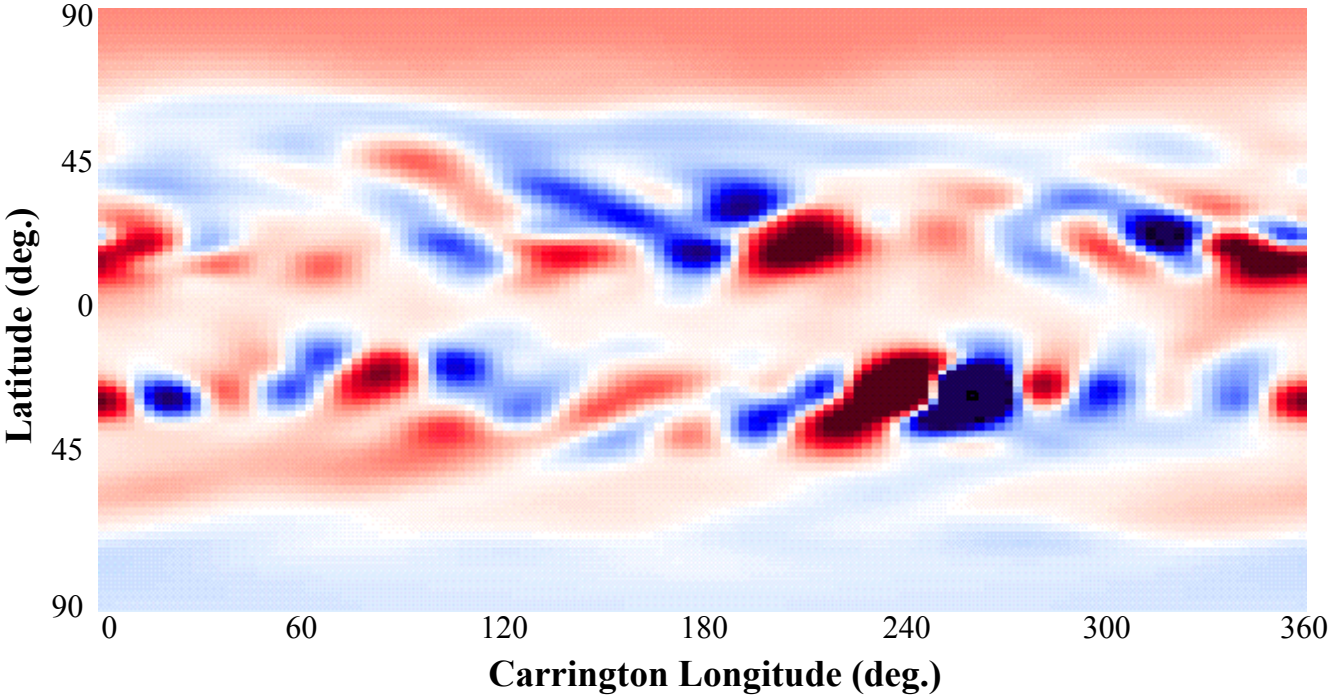

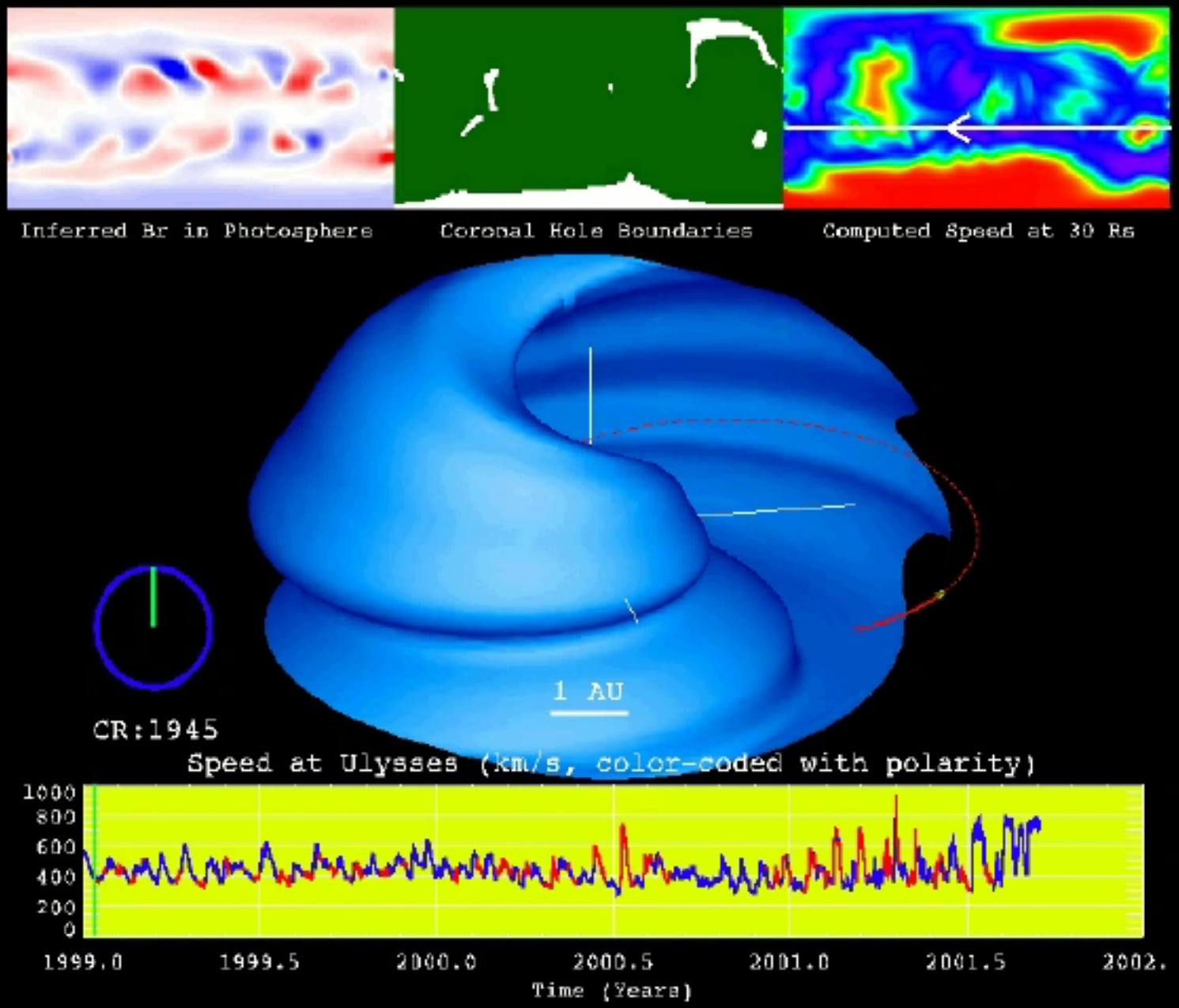
Inferred Br in Photosphere
Coronal Hole Boundaries
Computed Speed at 30 Rs
1 AU
CR:1945
Speed at Ulysses (km/s, color-coded with polarity)
1000
800
600
400
200
0
1999.0
1999.5
2000.0
2000.5
2001.0
2001.5
2002.
Time (Years)

EUV EMISSION

- The emission in the corona is dominated by collisional excitation from electron impact, so that the apparent emission rate is

$$R_{EUV} \propto \int_{\text{los}} n_e^2 f(T)\, dl \quad ,$$

where $f(T)$ is a (known) function that depends on coronal ion abundances, the line being observed, and the properties of the observing instrument (e.g., the Fe XII 195Å line for EIT)

Quantitative Comparison Between Observed and Computed Coronal Emission

SOHO/EIT and Yohkoh/SXT Observations on August 27, 1996

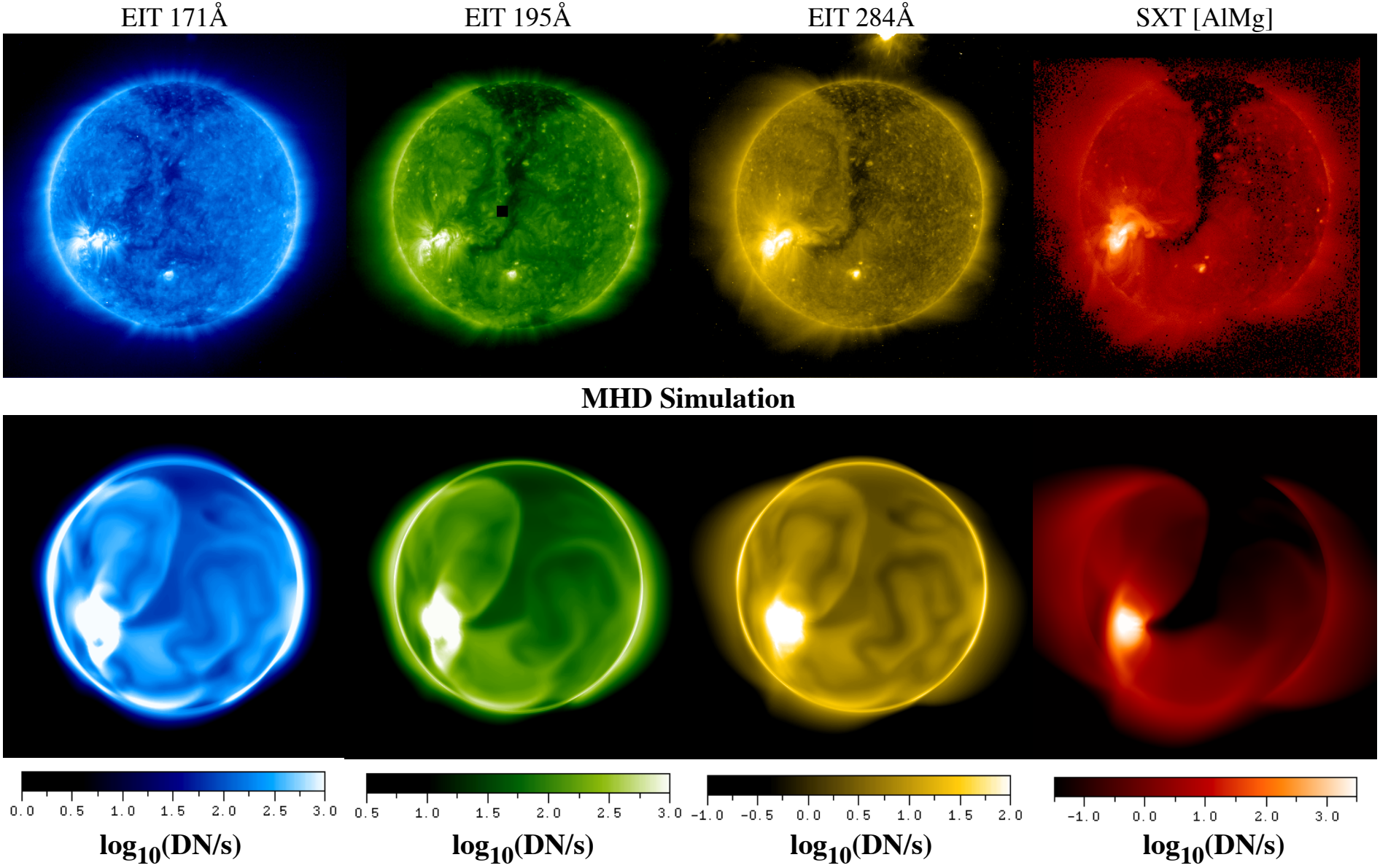

Comparing Emission from a Force-Free Magnetic Field Model with Observations of AR7986 on August 29, 1996

Magnetic Field Lines

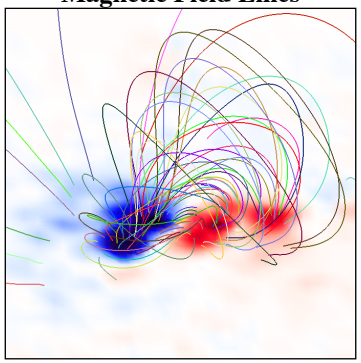

Normal Magnetic Field

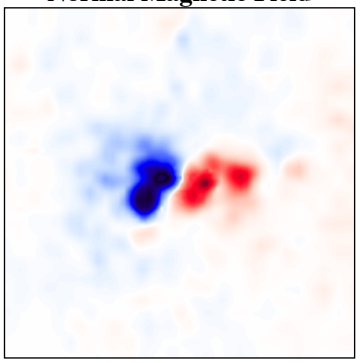

Simulated SXT Emission

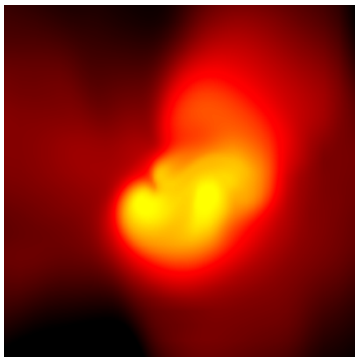

Simulated 171Å Emission

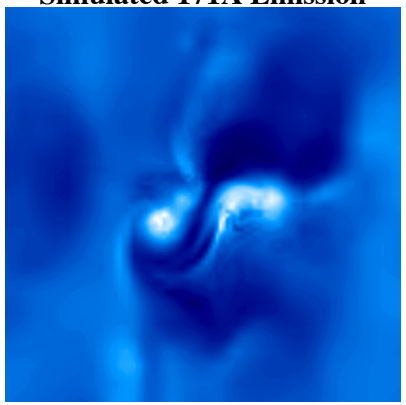

Simulated 195Å Emission

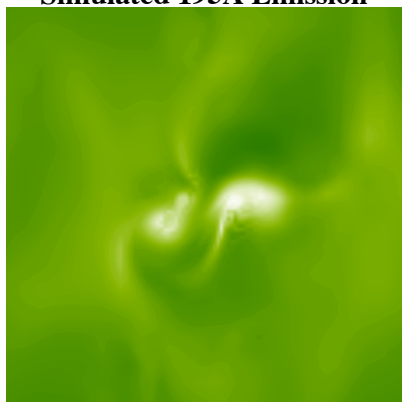

Simulated 284Å Emission

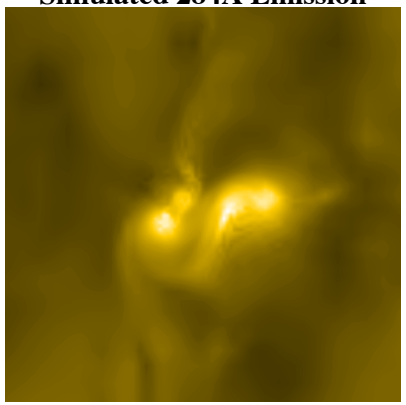

Observed EIT 171Å Emission

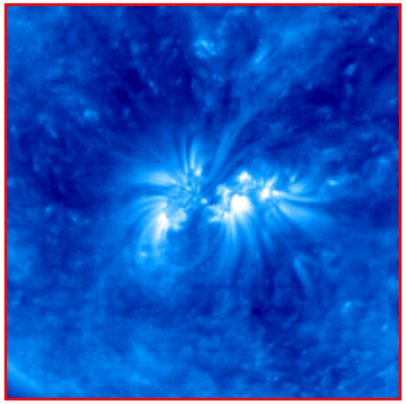

Observed EIT 195Å Emission

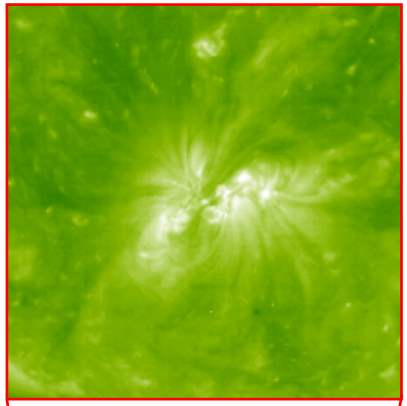

Observed EIT 284Å Emission

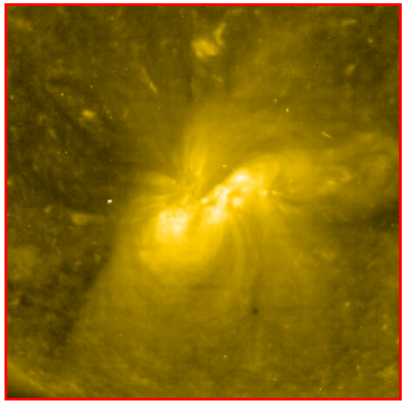

Observed EIT 171Å Emission

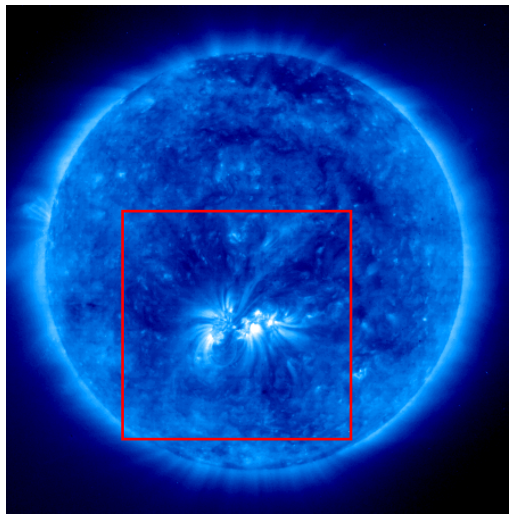

Observed EIT 195Å Emission

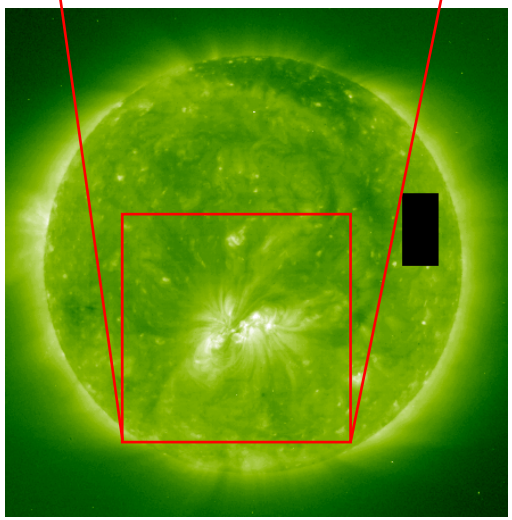

Observed EIT 284Å Emission

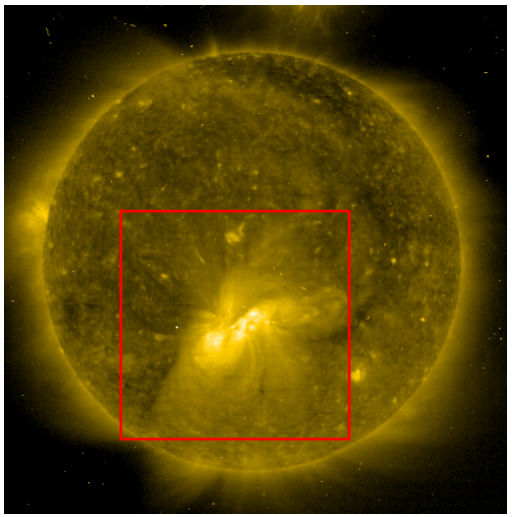

INPUTS/OUTPUTS

- **Inputs:**
  - A sequence of synoptic magnetic field maps (Kitt Peak, WSO, Mt. Wilson, MDI)
  - Polytropic: base temperature and density
  - Improved energy model: coronal heating distribution, Alfvén wave flux at base
- **Outputs:**
  - $\mathbf{B}(\mathbf{x})$, $\mathbf{v}(\mathbf{x})$, $T(\mathbf{x})$, $n(\mathbf{x})$
  - Field line traces, mapping, and connectivity
  - Field line structure and topology (K, Q, coronal hole maps)
  - Coronal hole maps
  - Heliospheric current sheet
  - Polarization brightness
  - EUV and X-ray emission
  - Alfvén and sound speed

TYPICAL RUN TIMES

- A low resolution run (with $71 \times 71 \times 64$ mesh points) takes several hours on a single-CPU machine
- An intermediate resolution run (with $101 \times 101 \times 128$ mesh points) takes several days on a single-CPU machine
- An intermediate resolution run takes many hours on a 64-CPU Beowulf cluster
- A high resolution run (with $200 \times 200 \times 300$ mesh points) takes several days on a supercomputer with 1000 processors

CAPABIILITIES

- **Present:**
  - Uses longitudinal magnetograms
  - Polytropic model (coronal + heliospheric)
  - Improved energy equation model
  - Flux evolution
- **Future:**
  - Incorporating vector magnetograms
  - Refinement of coronal heating specification (ongoing)
  - Two-temperature model (long term)

USING A SEQUENCE OF VECTOR MAGNETOGRAMS

- Boundary tangential electric field (definition):

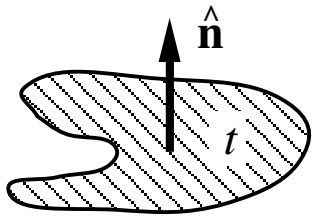

$$\mathbf{E}_t = \nabla_t \times (\Psi \hat{\mathbf{n}}) - \nabla_t \Phi$$

- Evolution of the normal boundary magnetic field, B_n:

$$\frac{1}{c}\frac{\partial B_n}{\partial t} = -\hat{\mathbf{n}}\cdot\nabla_t \times \mathbf{E}_t = \nabla_t^2 \Psi$$

$\Rightarrow$ A sequence of magnetograms can be used to determine Ψ

- Evolution of the normal boundary current density, J_n:

$$\frac{\partial \Phi}{\partial t} = \frac{\eta\, l}{\tau_{RC}}(J_n^{\mathrm{o}} - J_n)$$

where: l is the scale length of the active region (input)

τ_{RC} is the R–C time for the capacitor controlling the current source J_n^{o} (input)

$J_n^{\mathrm{o}} = \frac{c}{4\pi}\hat{\mathbf{n}}\cdot\nabla_t \times \mathbf{B}_t$ is deduced from a sequence of vector magnetograms